Dalton Transactions

ROYAL SOCIETY OF CHEMISTRY

FRONTIER

View Article Online
View Journal | View Issue

Cite this: *Dalton Trans.*, 2025, **54**, 4432

Received 22nd December 2024,
Accepted 21st January 2025

DOI: 10.1039/d4dt03517h

rsc.li/dalton

Recent advances in antiaromatic metallacycles

Lei Li,[a] Yang Li,[b] Wenfeng Jiang[a] and Wei Bai *[a]

Several antiaromatic metallacycles have been reported in the past 5 years, opening an emerging area of (anti)aromaticity and organometallic chemistry. In this work, we briefly review the synthesis and characterization of these complexes. Generally, experimental criteria, including planarity, bond length alternation, NMR chemical shift, chemical transformation, and theoretical criteria, mainly involving NICS, AICD, ASE or ISE, are applied for the antiaromaticity judgement.

Aromaticity is a fundamental concept in chemistry and is still under development. It has attracted continuing attention from chemists for 200 years since the isolation of benzene by Faraday in 1825.[1] Hückel's rule was first proposed to determine the aromaticity for cyclic planar conjugated hydrocarbons with $[4n + 2]$ π electrons,[2] while Breslow raised antiaromaticity for a system with $[4n]$ π electrons,[3] as a complement of aromaticity. One of the most significant features for aromatic compounds is their anomalous stability. In contrast, antiaromatic species are thermodynamically unstable and reactive, and their synthesis and characterization are challenging. For example, a sterically protected strategy was applied to construct substituted cyclobutadienes,[4] as the classic Hückel antiaromatic cyclobutadiene (Fig. 1a) was highly reactive and underwent fast Diels–Alder dimerization.

As an important class of aromatics, metallaaromatics have been extensively studied over 40 years since the prediction of the existence of metallabenzenes by Thorn and Hoffman in 1979.[5] Novel structures, such as metallabenzene, metallabenzyne, metallapentalene, metallacyclopropene, and spiro metalloles, have been reported.[6–12] Interestingly, the introduction of metal fragments into conjugated structures can also generate antiaromaticity. The isolation and reactivity of antiaromatic beryllole containing 4π electrons were demonstrated in 2020 (Fig. 1b).[13] Since then, several antiaromatic metallacycles of transition metals (Os, Ir, and Pt) have been synthesized and characterized (Fig. 1b).[14–19] These findings open a new area of antiaromatic and organometallic chemistry.

Braunschweig, Engels and coworkers presented the synthesis and isolation of the Lewis-base-stabilized beryllole **1** (Fig. 2), which contained a BeC_4 ring as a combination of a 4π-electron $[C_4Ph_4]$ fragment with a neutral, zero π-electron carbene-stabilized beryllium fragment.[13] Single-crystal X-ray diffraction confirmed the solid-state structure of **1**, as well as the effective planarity (the deviations of the BeC_4 atoms from the calculated least-squares ring plane, 0.021–0.094 Å) and significant bond-length alternations (C–C distance, 1.512(2) Å; C=C distances, 1.359(2) and 1.358(2) Å) of the beryllole (BeC_4) ring. The nucleus independent chemical shift (NICS)[20,21] calculations showed that the $NICS_{zz}(1)$ and $NICS_{zz}(-1)$ values at a point 1 Å above and below the BeC_4 ring plane were +14.1 and +13.5 ppm, respectively, suggesting antiaromaticity. NICS is a commonly used theoretical method based on electromagnetic properties to study aromaticity. If the NICS value is positive, the system is probably antiaromatic and *vice versa* for aromatic structures. NICS values of some antiaromatic organics are given in Fig. 1a.[22–24] Furthermore, the ring exhibited counterclockwisely paratropic circulation in the anisotropy of the

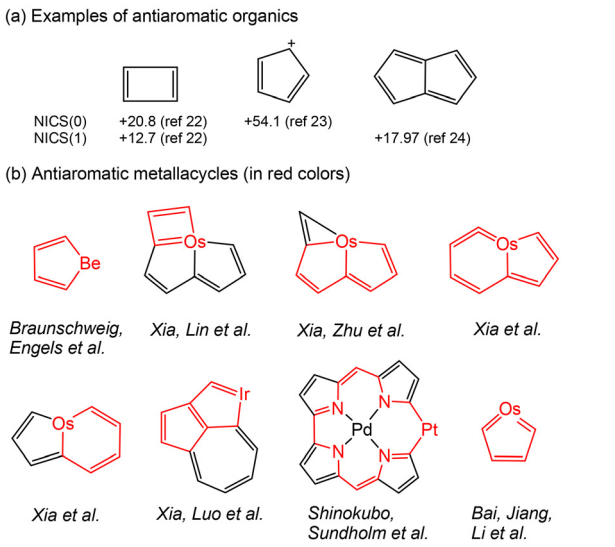

Fig. 1 Examples of antiaromatics.

[a]*School of Chemistry, Dalian University of Technology, Dalian 116024, P.R. China. E-mail: baiwei@dlut.edu.cn*
[b]*School of Chemical Engineering, Ocean and Life Sciences, Dalian University of Technology, Panjin 124221, P.R. China*

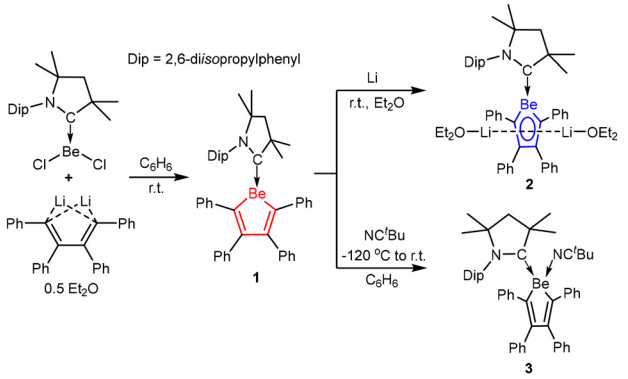

Fig. 2 Synthesis of antiaromatic beryllole **1** and its reactivity.

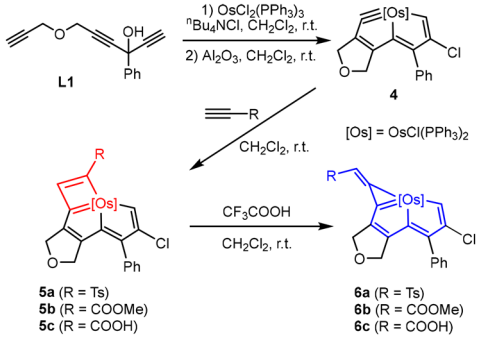

Fig. 3 Synthesis of antiaromatic osmacyclobutadienes **5a–c** and their reactivity.

induced current density (AICD) analysis, which was characteristic of antiaromatic systems.[25,26] AICD is a qualitative visualization method to investigate aromaticity, concerning also the electromagnetic characteristics. Aromatic rings will generate diatropic ring currents towards an applied magnetic field. Aromatic stabilization energy (ASE)[27,28] is an energy-based theoretical criterion, and belongs to the isomerization stabilization energy (ISE) of an isodesmic reaction.[29,30] Positive ASE values are related to the stability of aromatic compounds due to cyclic delocalization. Thus the negative ASE value (−7.8 kcal mol^{-1}) of model structures indicated the destabilization of cyclic localization and supported the antiaromatic property of the 4-electron BeC_4 π system in **1**. The authors proved that the ring systems $C_5H_5^+$ and BC_4H_5 were far more antiaromatic than the simplified structure of **1**, in which Ph groups were replaced by H atoms. The conversion of antiaromatic beryllole **1** to aromatic and non-aromatic compounds were demonstrated. As shown in Fig. 2, chemical reduction of **1** with lithium sand produced aromatic beryllole **2**, a kind of dianion metallole,[6,7] while the addition of a second Lewis donor NC^tBu generated non-aromatic (negligibly antiaromatic) beryllole **3**.

Through the bridgehead replacement of fused structures with a transition metal fragment, numerous metallaaromatics have been constructed.[6–11] In 2021, Xia, Zhu and coworkers presented the unprecedented synthesis of osmium-bridgehead naphthalene featuring a highly twisted structure.[31] They found that such a conformation worked together with the phosphonium substituents on the rings to release the antiaromaticity in the planar metal-bridgehead naphthalene structure.

In 2022, Xia, Lin and coworkers obtained fused osmacyclobutadiene complexes **5a–c** in high yields (>90%) from the [2 + 2] cycloaddition reactions of terminal alkynes with osmapentalyne **4**, which was synthesized from a mixture of $OsCl_2(PPh_3)_3$ and multiyne **L1** in the presence of excess tetrabutylammonium chloride (Fig. 3).[14] Single-crystal X-ray diffraction analysis revealed the tricyclic structure of **5a**, its planarity (the mean deviation from the calculated least-squares plane of the metallacyclobutadiene ring, 0.022 Å), and notable bond alternations (C–C distances, 1.338(5) and 1.425(4) Å; Os–C distances, 2.064(3) and 2.218(3) Å) in the four-membered metallacyclobutadiene ring. Theoretical calculations were performed on the simplified model of **5a**, indicating the antiaromaticity of the metallacyclobutadiene unit with a positive $NICS_{zz}(1)$ value and distinct counterclockwise circulation from AICD. Canonical molecular orbital (CMO) NICS and electron localization function (ELF_π) basins calculations further analysed the π contributions to the antiaromaticity.[32] Zhu's group studied similar organometallic fragments in 2016, and they found unexpected higher stabilization and weaker antiaromaticity of ruthenapentalocyclobutadienes compared to those of their osmium counterparts.[33] In the presence of CF_3COOH, aromatic complexes **6a–c** were isolated in moderate yields from antiaromatic complexes **5a–c** (Fig. 3). This unusual acid-induced ring contraction of metallacyclobutadiene to metallacyclopropene *via* a ring opening–reclosing process was driven by π- and σ-aromaticity relay. The authors investigated the mechanism both theoretically and experimentally.

In the same year, Xia, Zhu and coworkers reported the first examples of planar Craig-type antiaromatic species with [4*n* + 2] π electrons, as a complement of the development of π-aromaticity and antiaromaticity.[15] As shown in Fig. 4, aromatic osmapentalene complexes **7** could be deprotonated to generate the corresponding antiaromatic complexes **8** in good yields. The crystal structures of **7a**, **7a-bpy**, **7b-bpy**, **7c**, **8a**, **8b**, **8a-bpy** and **8b-bpy** were determined by single-crystal X-ray diffraction, and were found to have planar conjugated systems (the mean deviations from the calculated least-squares plane of the **5MR**s: 0.028 Å for **7a**, 0.027 Å for **7a-bpy**, 0.016 Å for **7b-bpy**, 0.023 Å for **8a-PPh$_3$**, 0.023 Å for **8b-PPh$_3$**, 0.052 Å for **8a-bpy** and 0.061 Å for **8b-bpy**). Generally, the fused five-membered rings in complexes **7** showed negligible bond alternations, while significant alternations in the bond lengths were observed in complexes **8**. The delocalized structures of **7** indicated aromaticity and the localized structures of **8** suggested possible antiaromaticity. The NMR data and UV-Vis-NIR absorption spectra of complexes **8** also demonstrated antiaromatic characters. NICS, AICD, the iso-chemical shielding surface (ICSS),[34] isomerization stabilization energy, and electron density of delocalized bond (EDDB)[35] calculations were

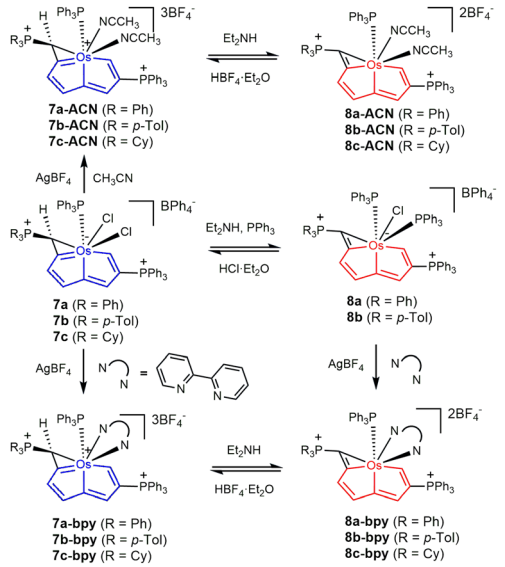

Fig. 4 Synthesis of antiaromatic complexes **8** and their reactivity.

performed to investigate the antiaromaticity of **8**. The analysis of its electronic structure pointed out that five occupied π molecular orbitals (π-MOs) formed an eight-center ten-electron (**8c–10e**) Craig antiaromatic system. Complexes **8** were easily protonated back to **7**. Further experimental and theoretical studies revealed that the highly exothermic acid–base neutralisation process was the driving force for the realization of Craig antiaromatic compounds, and a higher acidity of complexes **7** favored this conversion.

In 2023, a highly strained antiaromatic metallacycle (**9**) with a cyclic metal vinylidene unit was isolated and characterized by Xia's group (Fig. 5).[16] Single-crystal X-ray diffraction analysis confirmed the fused iso-metallabenzene structure with distinctive single–double C–C bond alternations. The strain in the bent metal vinylidene structure and antiaromaticity of the osmabicycle in **9** were evaluated by computational studies. Notably, the presence of a transition metal reduced the high ring strain, and the involvement of phosphonium substituents assisted in the stabilization of antiaromatic systems. Complex

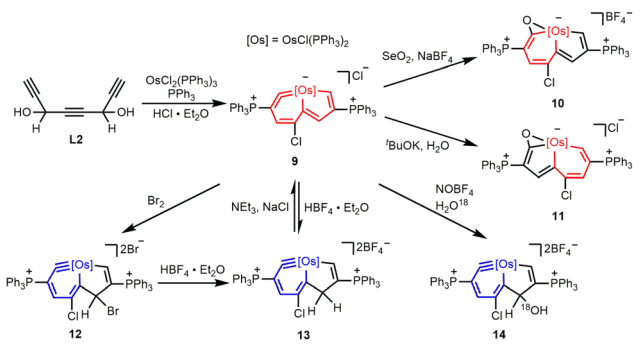

Fig. 5 Synthesis of antiaromatic complexes **9–11** and the reactivity of **9**.

9 could be oxidized to **10** and **11** with ring reshuffling (Fig. 5). The osmacyclohexadiene rings were also antiaromatic. Treatment of antiaromatic **9** with electrophiles, *i.e.* bromine (Br_2) and tetrafluoroboric acid (HBF_4), afforded the corresponding metallaindynes **12** and **13**, respectively, both of which contained an aromatic osmabenzyne unit (Fig. 5). **14** with a similar structure was formed with the addition of nitrosonium tetrafluoroborate ($NOBF_4$) in the presence of H_2O (Fig. 5). Furthermore, the antiaromatic–aromatic switching between **9** and **13** was smoothly induced by an acid (HBF_4) and base (NEt_3), which could be utilized to construct switchable optical materials.

In the same year, Shinokubo, Sundholm and coworkers reported the synthesis of a Pd(II) 10-platinacorrole complex with a norbornadiene (NBD) ligand (**17**) from ligand substitution of cyclooctadiene (COD) **16** (Fig. 6).[17] Single-crystal X-ray diffraction analysis showed the distorted structure of complex **16** and the planar structure of complex **17** (the mean deviations from the calculated least-squares ring plane: 0.229 Å for **16** and 0.098 Å for **17**). The marginally positive NICS(1) values (about +3 ppm) suggested that the COD complex **16** is nonaromatic, while the unique antiaromaticity of **17** was confirmed by positive NICS(1) values (8.4 to 11.5 ppm) and a substantial paratropic ring current from GIMIC. The UV-Vis-NIR absorption spectra of **16** exhibited a broad absorption band from 700 to 1000 nm, whereas broad and weak absorption bands tailing to 1500 nm were observed for the antiaromatic complex **17** due to effective π-conjugation. In the MOs of a simplified model of **17**, two d orbitals (d_{zx} and d_{yz}) on the Pt center effectively overlapped with the π orbitals of the tetrapyrrole unit, thus formally creating a cyclic 20π-conjugated system along the inner circle (Fig. 6).

In 2024, Xia, Luo and coworkers synthesized a new type of nonalternant analogue of pentacene that incorporated a non-terminal azulene unit and a conjugated metallacycle.[18] Treatment of iridacyclopentadiene **18** with terminal aryl alkynes and $AgBF_4$ in the presence of $HBF_4{\cdot}Et_2O$ produced complexes **19** (Fig. 7). Single-crystal X-ray diffraction analysis revealed the structure of **19a**, which contained an azulene-fused acene fused with a conjugated five-membered metallacycle. The NICS (+5.1 and +7.2 ppm) and AICD (paratropic ring currents with counterclockwise vectors) results suggested weak antiaromaticity in the five-membered rings (Fig. 7). Enhanced absorptions of complexes **19** in the low-energy regions were observed, attributed to the extensive conjugated aryl substituents that shift the HOMOs of acenes and narrow the HOMO–

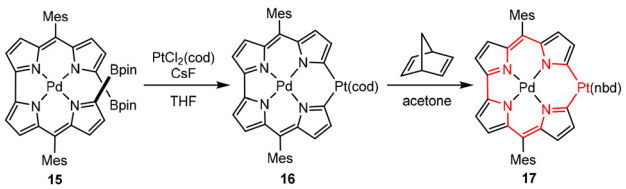

Fig. 6 Synthesis of the antiaromatic complex **17**.

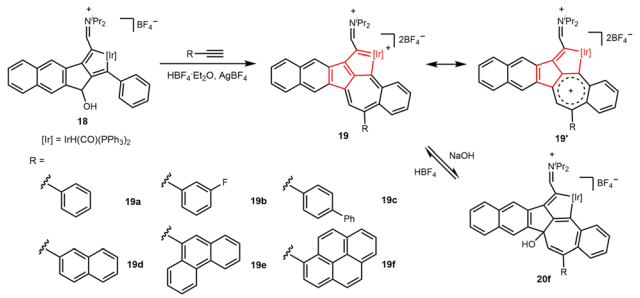

Fig. 7 Synthesis of antiaromatic complexes **19** and their reactivity.

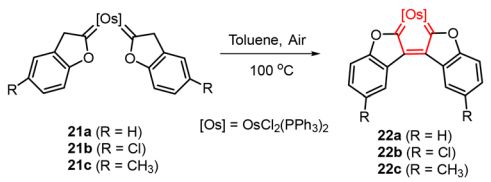

Fig. 8 Synthesis of antiaromatic osmacyclopentatrienes **22**.

LUMO energy gap. The yellow-green solution of **19f** turned red immediately after the addition of NaOH, resulting in **20f** quantitatively. Reversible base–acid stimuli responsiveness was achieved between **19f** and **20f**, which provide the potential for future applications in switchable photofunctional materials.

Recently, Bai, Jiang, Li and coworkers studied the (anti)aromatic properties of metallacyclopentatriene complexes MC_4R_4 for the first time.[19] The authors synthesized osmacyclopentatrienes **22** from oxidative dehydrogenation of novel *cis*-biscarbene complexes **21** (Fig. 8), which were obtained from a mixture of $OsCl_2(PPh_3)_3$ and 2-(trimethylsilyl)ethynyl phenols.[19] The solid structure of **22a** was determined by single-crystal X-ray diffraction, containing a fused pentacyclic boomerang-like structure with a localized five-membered OsC_4 ring in the centre. Unlike the above antiaromatic metallacycles, complexes **22** were relatively stable and appeared unreactive under different conditions. The antiaromaticity of the osmacyclopentatriene unit was verified by various theoretical indices, including NICS, AICD, GIMIC, and ISE calculations. The UV-Vis absorption spectra of **22** showed weak and broad absorption band tails at 750–800 nm due to the narrow HOMO–LUMO gap in antiaromatic systems. The electronic structure analysis predicted that three occupied π-MOs formed a **5c–6e** Craig antiaromatic system. This work provides new insight into the discovery of antiaromatic species. For instance, localized structures such as metallacyclopentatriene may be antiaromatic instead of merely nonaromatic.

Conclusion and outlook

In this frontier article, we have summarized the recent progress in the development of antiaromatic metallacycles. Both experimental and theoretical characterization has been applied. Structurally, planar localized rings exhibit a characteristic feature of pronounced single and double C–C bond alternations. Magnetically, NMR chemical shift comparisons with aromatic or nonaromatic analogues are noticeable. Moreover, NICS and AICD are commonly used electromagnetic indexes. Energetically, ISE and ASE calculations show favourably exothermic changes with the destruction of conjugated antiaromatic rings. Choosing appropriate aromaticity indexes is particularly important to evaluate the (anti)aromaticity.[36] Hückel antiaromatics have $[4n]$ π electrons, while Craig ones have $[4n + 2]$ π electrons. Most of the antiaromatic metallacycles can be further converted to nonaromatic or aromatic species, producing fascinating structures. In particular, acid–base induced transformations with photo-responsive behaviour have materials applications. This emerging area in both (anti)aromaticity and organometallic chemistry is expected to yield intriguing and surprising structures, reactions, and possibilities.

Data availability

There are no new data to report in this frontier article.

Conflicts of interest

There are no conflicts to declare.

Acknowledgements

This work was supported by the National Natural Science Foundation of China (Grant No. 22001030 and 21903010) and Dalian University of Technology.

References

1 M. Faraday, *Philos. Trans. R. Soc. London*, 1825, **115**, 440–466.
2 E. Hückel, *Z. Phys.*, 1931, **70**, 204–286.
3 R. Breslow, *Acc. Chem. Res.*, 1973, **6**, 393–398.
4 H. Kimling and A. Krebs, *Angew. Chem., Int. Ed. Engl.*, 1972, **11**, 932–933.
5 D. L. Thorn and R. Hoffmann, *Nouv. J. Chim.*, 1979, **3**, 39–45.
6 Y. Zhang, C. Yu, Z. Huang, W. Zhang, S. Ye, J. Wei and Z. Xi, *Acc. Chem. Res.*, 2021, **54**, 2323–2333.
7 D. Chen, Y. Hua and H. Xia, *Chem. Rev.*, 2020, **120**, 12994–13086.
8 I. Fernández, G. Frenking and G. Merino, *Chem. Soc. Rev.*, 2015, **44**, 6452–6463.
9 B. J. Frogley and L. J. Wright, *Coord. Chem. Rev.*, 2014, **270–271**, 151–166.
10 J. Chen and G. Jia, *Coord. Chem. Rev.*, 2013, **257**, 2491–2521.

11 B. Fu, W. Bai, Y. Li and W. Jiang, *Chem. Commun.*, 2024, **60**, 12816–12829.
12 D. Chen, Q. Xie and J. Zhu, *Acc. Chem. Res.*, 2019, **52**, 1449–1460.
13 D. K. Roy, T. Trçster, F. Fantuzzi, R. D. Dewhurst, C. Lenczyk, K. Radacki, C. Pranckevicius, B. Engels and H. Braunschweig, *Angew. Chem., Int. Ed.*, 2021, **60**, 3812–3819.
14 K. Zhuo, Y. Liu, K. Ruan, Y. Hua, Y. Lin and H. Xia, *Nat. Synth.*, 2023, **2**, 67–75.
15 L. Chen, L. Lin, A. R. Nath, Q. Zhu, Z. Chen, J. Wu, H. Wang, Q. Li, W. Lin, J. Zhu and H. Xia, *Proc. Natl. Acad. Sci. U. S. A.*, 2023, **120**, e2215900120.
16 Q. Li, Y. Hua, C. Tang, D. Chen, M. Luo and H. Xia, *J. Am. Chem. Soc.*, 2023, **145**, 7580–7591.
17 K. Miwa, T. Yokota, Q. Wang, T. Sakurai, H. Fliegl, D. Sundholm and H. Shinokubo, *J. Am. Chem. Soc.*, 2024, **146**, 1396–1402.
18 Y. He, Y. Zhu, M. Luo and H. Xia, *Chin. Chem. Lett*, 2024, 110463.
19 B. Fu, Y. Wang, Y. Zhao, Y. Li, W. Jiang and W. Bai, *J. Am. Chem. Soc.*, 2024, **146**, 30790–30795.
20 P. von R. Schleyer, C. Maerker, A. Dransfeld, H. Jiao and N. J. R. van Eikema Hommes, *J. Am. Chem. Soc.*, 1996, **118**, 6317–6318.
21 D. Geuenich, K. Hess, F. Köhler and R. Herges, *Chem. Rev.*, 2005, **105**, 3758–3772.
22 P. von R. Schleyer, M. Manoharan, Z.-X. Wang, B. Kiran, H. Jiao, R. Puchta and N. J. R. van Eikema Hommes, *Org. Lett.*, 2001, **3**, 2465–2468.
23 H. Jiao, P. von R. Schleyer, Y. Mo, M. A. McAllister and T. T. Tidwell, *J. Am. Chem. Soc.*, 1997, **119**, 7075–7083.
24 C. A. Barboza, E. Barboza, R. Arratia-Perez and D. M. Carey, *Chem. Phys. Lett.*, 2012, **545**, 88–94.
25 R. Herges and D. Geuenich, *J. Phys. Chem. A*, 2001, **105**, 3214–3220.
26 Z. Chen, C. S. Wannere, C. Corminboeuf, R. Puchta and P. V. R. Schleyer, *Chem. Rev.*, 2005, **105**, 3842–3888.
27 P. V. R. Schleyer, H. Jiao, B. Goldfuss and P. K. Freeman, *Angew. Chem., Int. Ed. Engl.*, 1995, **34**, 337–340.
28 M. K. Cyrański, P. V. R. Schleyer, T. M. Krygowski, H. Jiao and G. Hohlneicher, *Tetrahedron*, 2003, **59**, 1657–1665.
29 P. V. R. Schleyer and F. Pühlhofer, *Org. Lett.*, 2002, **4**, 2873–2876.
30 C. S. Wannere, D. Moran, N. L. Allinger, B. A. Hess, L. J. Schaad and P. V. R. Schleyer, *Org. Lett.*, 2003, **5**, 2983–2986.
31 C. Tang, Y. Zhao, J. Wu, Z. Chen, L. Liu, Y. Tan, J. Zhu and H. Xia, *J. Am. Chem. Soc.*, 2021, **143**, 15587–15592.
32 J. C. Santos, W. Tiznado, R. Contreras and P. Fuentealba, *J. Chem. Phys.*, 2004, **120**, 1670–1673.
33 J. Wu, Y. Hao, K. An and J. Zhu, *Chem. Commun.*, 2016, **52**, 272–275.
34 S. Klod and E. Kleinpeter, *J. Chem. Soc., Perkin Trans.*, 2001, **2**, 1893–1898.
35 D. W. Szczepanik, M. Andrzejak, K. Dyduch, E. Zak, M. Makowski, G. Mazur and J. Mrozek, *Phys. Chem. Chem. Phys.*, 2014, **16**, 20514–20523.
36 Q. Zhu, S. Chen, D. Chen, L. Lin, K. Xiao, L. Zhao, M. Solàd and J. Zhu, *Fundam. Res.*, 2023, **3**, 926–938.